Published online 26 November 2007

Nucleic Acids Research, 2008, Vol. 36, No. 2 ***387–392***
doi:10.1093/nar/gkm1024

Intracellular expression profiles measured by real-time PCR tomography in the *Xenopus laevis* oocyte

Radek Sindelka[1], Jiri Jonák[1,4], Rebecca Hands[2], Stephen A. Bustin[2] and Mikael Kubista[1,3,*]

[1]Laboratory of Gene Expression, Institute of Molecular Genetics, Academy of Sciences of the Czech Republic, Videnska 1083, 14220 Prague 4, Czech Republic, [2]Barts and the London Queen Mary's School of Medicine and Dentistry, Academic Surgery, London, E1 1BB, UK, [3]TATAA Biocenter, Medicinargatan 8A, 413 46 Göteborg, Sweden and [4]Institute of Medical Biochemistry, First Medical Faculty, Charles University, Katerinska 1083, 12000 Prague 2, Czech Republic

Received October 9, 2007; Revised October 27, 2007; Accepted October 28, 2007

ABSTRACT

Real-time PCR tomography is a novel, quantitative method for measuring localized RNA expression profiles within single cells. We demonstrate its usefulness by dissecting an oocyte from *Xenopus laevis* into slices along its animal–vegetal axis, extracting its RNA and measuring the levels of 18 selected mRNAs by real-time RT-PCR. This identified two classes of mRNA, one preferentially located towards the animal, the other towards the vegetal pole. mRNAs within each group show comparable intracellular gradients, suggesting they are produced by similar mechanisms. The polarization is substantial, though not extreme, with around 5% of vegetal gene mRNA molecules detected at the animal pole, and around 50% of the molecules in the far most vegetal section. Most animal pole mRNAs were found in the second section from the animal pole and in the central section, which is where the nucleus is located. mRNA expression profiles did not change following *in vitro* fertilization and we conclude that the cortical rotation that follows fertilization has no detectable effect on intracellular mRNA gradients.

INTRODUCTION

A single egg contains all the information required for its proliferation and differentiation into a complete organism and accurate spatial distribution of maternal factors is a critical issue for early development, cell determination, differentiation and germ layers formation (1). All mRNAs translated during the initial stages of development originate from the mother as transcription of new zygotic mRNA is initiated only after 12 cell divisions during what is called the midblastula transition (MBT).

The cellular distribution of maternal factors and their functions are usually studied in model organisms such as *Drosophila melanogaster*, *Caenorhabditis elegans* and *Mus musculus*. These studies are hampered by the very small amounts of RNA (~pg of total RNA) in invertebrate and mammalian cells. In contrast, the egg from the African clawed frog *Xenopus laevis* contains a microgram of total RNA. Furthermore, two differently coloured hemispheres can easily be distinguished in *Xenopus* eggs. The colouration difference identifies the first developmental animal–vegetal, A–V, axis, which is formed during mid- and late stages of oogenesis. The dark pigmented animal hemisphere derives its colour from the pigmented melanosomes and contains the egg nucleus (2), whereas the opposite light vegetal hemisphere contains yolk platelets. During early development, the animal hemisphere is transformed into ectodermal cells with epidermis and neural fate. The vegetal hemisphere follows endodermal fate (gut) and the marginal zone forms mesoderm layer with blood, bone and muscle cell types.

Maternal factors are distributed along the A–V axis during oogenesis and have many different roles in *Xenopus* early development. Some are transcription factors, while others are signalling factors or regulators of activity of signalling molecules (3). Two groups of mRNA molecules have been reported to localize in the vegetal hemisphere during oogenesis. Germ cell determinants such as Xcad2 (Nanos related, Zn finger protein), Xpat (unknown function), DeadSouth (RNA helicase) and mRNAs for the Wnt11 (Wnt family member) gene are vegetally localized in early stages 1 and 2 by the METRO

*To whom correspondence should be addressed. Tel: +46 31 741 18 00; Fax: +46 31 741 17 01; Email: mikael.kubista@img.cas.cz

(messenger transport organizer) pathway (2–8). A second group of vegetal genes includes VegT (T-box transcription factor), Otx1 (a homeobox gene) and Vg1 (TGF-beta family member). These localize vegetally by cytoskeletal-based transportation during later stages of oogenesis (8,9). Other genes, such as Oct60 (transcription factor, POU family), An1 (Ubiquitin like fusion protein), An2 (Mitochondrial ATPase subunit), Ets1 and Ets2 (transcription factors, ETS family members) and XPar-1 (serine/threonine kinase) have been found localized to the animal pole (3,9–11). The mechanism behind this specific localization is not well understood.

During fertilization, *Xenopus* sperm enters the egg through the animal hemisphere and the point of entry can be distinguished by a change in cortex cytoskeleton structure that leads to a local change in pigmentation. The process, called cortical rotation, occurs some 25 min after fertilization. The cortex rotates by about 30° and alters A–V organization through cytoskeletal and cytoplasmic rearrangements (12,13). The cortex movement induces local redistribution of β-catenin protein and the β-catenin stabilizing agent to a site opposite to the sperm's entrance (14,15). Accumulated β-catenin proteins then induce local gene expression of some zygotic factors including siamois and Xnr3. These are important for the formation of the organizer, which defines the future dorsal site of the embryo.

We have previously shown that there is substantial variation in gene expression among seemingly homogeneous cells (16). In this work we describe a novel approach to study intracellular expression profiles by real-time PCR tomography (17,18).

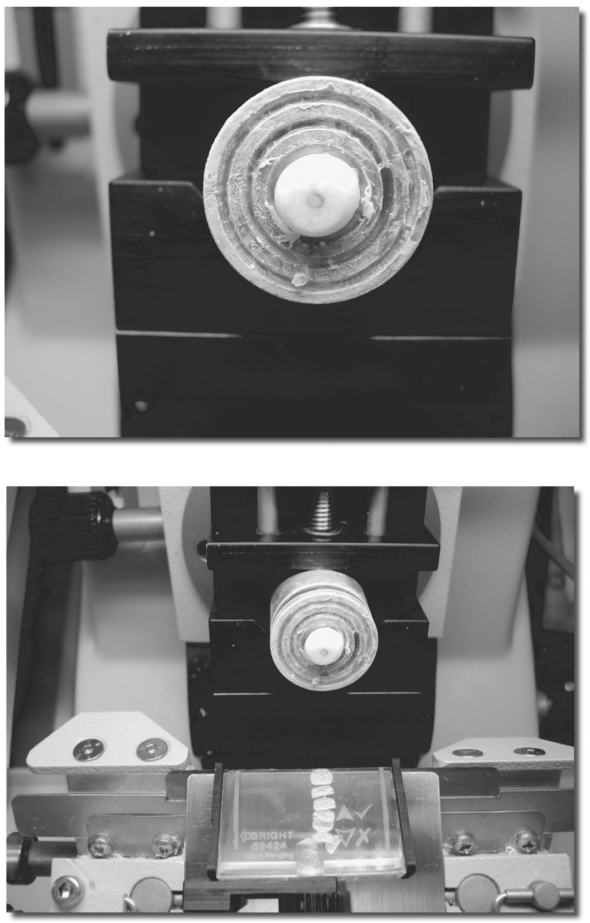

Figure 1. Photographs showing the process of preparing material for real-time PCR tomography. (**A**) The *Xenopus laevis* oocyte imbedded in OCT is mounted in a cryostat. (**B**) The material is sliced for subsequent analysis by real-time RT-PCR.

MATERIALS AND METHODS

Xenopus laevis females were stimulated by hCG (human chorionic gonadotrophin) injection and *in vitro* fertilized (IVF) eggs were incubated at 22°C. The eggs were not treated with cystein, which is common procedure, because the treatment compromises manipulation of the eggs and RNA stability after defrosting of the material. Only eggs that turned round with the animal pole on the top were harvested for sectioning. More than 90% of the turned eggs divided within 90 min following IVF. Four types of eggs were collected: unfertilized eggs and eggs collected at 25, 50 and 85 min post- IVF. First cell division occurs after 90 min. The collected eggs were frozen at –70°C and stored.

For analysis the eggs were embedded in optimum cutting temperature (OCT) compound and dissected into 35 slices (30 μm) across the A–V axis (Figure 1). Consecutive slices were pooled into five groups with seven slices in each. From each group, 200–500 ng of total RNA was extracted using RNeasy Micro kit (Qiagen). RNA concentrations were determined with the Nanodrop® ND1000 quantification system (Nanodrop Inc.) and RNA quality was assessed with the 2100 Bioanalyzer using the RNA Pico Chip (Agilent). In general RNA quality was very high. Total RNA was reverse transcribed (High Capacity cDNA Archive Kit- Applied Biosystems) using 100 ng total RNA with 2.5 μl of random primers in water in a total volume of 16.5 μl. The mixture was incubated for 10 min at 72°C. After cooling to room temperature, 1 μl of dNTPs (25×), 2.5 μl of 10× reverse transcription buffer and 2.5 μl of MultiScribeReverse Transriptase (50 U/μl) were added. The mixture was incubated for 2 h at 37°C. cDNA was diluted to a final volume of 100 μl. Real-time PCR assays had a final volume of 25 μl and contained 3 μl of cDNA, 1U SureStart *Taq* DNA polymerase (Stratagene-Europe), 2.5 μl of reaction buffer (10×), 3 mM $MgCl_2$, 0.4 mM dNTP mix, 50 000-fold diluted SYBRGreen I (Molecular Probes), 25 000-fold diluted ROX reference dye and 0.3 mM primers. PCR was run in a Mx3005P (Stratagene) with cycling conditions: 95°C for 12 min, 45 cycles at 95°C for 20 s, 60°C for 25 s, 72°C for 30 s. After cycling the samples were heated to 95°C for 1 min, and melting curve was recorded between 65 and 95°C.

Gene-expression data were analyzed using GenEx software from MultiD Analysis (www.multid.se) and Prism4 from Graphpad (www.graphpad.com). It was not possible to use any internal reference genes for normalization, since this is the first time intracellular mRNA

levels are being quantitated and there is no information on what mRNAs might be homogeneously distributed within the cell. Consequently, we normalized individual mRNAs against the total amount of RNA used for reverse transcription, essentially measuring gene-expression levels relative to the total amount of RNA in each section. Since RNA yield is rather uniform, we assume that total RNA is distributed homogenously in the cell. Consequently, normalization is against the volume of the segments, thus accounting for the differences in segment sizes due to the spherical shape of the cell. Although the data are perfectly comparable within each section, there may be bias across sections due to variations in the density of total RNA and in reverse transcription yields. These are caused by the sample matrix, which is quite different in the animal and the vegetal poles of the oocyte. The real-time PCR CT values were converted to relative quantities assuming 100% PCR efficiency, and the amounts of transcripts in the five egg sections were expressed as the fractions of the mRNA molecules found in each of five segments along the A–V axis in the *Xenopus* oocyte:

$$x_j = \frac{2^{-\mathrm{CT}_j}}{\sum_{i=1}^{5} 2^{-\mathrm{CT}_i}}$$

CT_j is the CT determined for section 'j' of the oocyte and x_j is the fraction of the mRNA found in this section. Since the amounts of mRNAs in the five sections are of the same order of magnitude, the assumption of 100% PCR efficiency will have little effect on the calculated intracellular mRNA profiles. The initial normalization against total RNA ensures that the profiles reflect true variations in the levels of the mRNAs along the A–V axis of the cell.

The conventional real-time PCR results were confirmed for selected genes with digital PCR using the BIOMARK digital array from Fluidigm (www.fluidigm.com). The array is designed to accept 12 sample mixtures, which each is partitioned into a different 765-chamber grid. One step RT–qPCR was performed directly on the chip. Ten-microliter reaction mix was loaded onto the chip, containing 3.4 µl of total RNA, 0.5 µl SuperScript RT/Taq (CellsDirect qPCR-RT kit, Invitrogen), 1 µl buffer containing ROX, 1 µl of primers (9 µM) and FAM-labelled TaqMan probe (2 µM) and 0.1 µl of Tween (10%). The input amount of total RNA was tuned to produce less cDNA molecules than the number of chambers. The mixture was distributed into the 765 chambers, incubated for 15 min at 50°C for reverse transcription and then analyzed by PCR, starting with HotStart activation at 95C° for 2 min followed by 45 PCR cycles at 95°C for 15 s and 60°C for 30 s. FAM/ROX fluorescence signal was collected at the end of each cycle, and the number of chambers that gave positive fluorescence signal after 40 cycles was registered. Assuming Poisson distribution of the cDNA molecules in the chambers, the average number of cDNA molecules per chambers is given by $\mathrm{In}\{[1-P(x\geq 1)]^{-1}\}$, where $P(x\geq 1)$ is the fraction of positive PCR reactions. A sample distributed into 765 chambers thus contained a total of $765\times \mathrm{In}\{[1-P(x\geq 1)]^{-1}\}$ cDNA molecules. The number of mRNA molecules in the sample can then be grossly estimated assuming 80% cDNA synthesis yield in the reverse transcription reaction (19).

RESULTS

Expression levels of mRNAs specified by the Wnt11, FoxH1, VegT, Vg1, Oct60, GSK-3β, dishevelled, elongation factor-1α (EF-1α), Xdazl, Xmam, Tcf-3, GAPDH, β-catenin, Xcad2, Otx1, XPar-1, Deadsouth and Stat3 genes were all characterized by distinct and reproducible intracellular gradients. As an example, Figure 2A and B shows Vg1 and Oct60 intracellular mRNA gradients measured on eggs from four different females. Oct60 is predominantly found at the animal pool, while Vg1 is preferably found at the vegetal pool. Although there is variation among individual cells, the intracellular gradients are clearly observed against the biological variation of the females, as reflected by the standard errors of the means. Figure 2C and D also shows mRNA intracellular distributions for Vg1 and Oct60 prior to IVF, and at 20, 55 and 85 min after IVF. Statistical analysis using two-way ANOVA with Bonferroni post-test on a pairwise comparison of the profile of the unfertilized oocyte with mRNA profiles collected at different time points after fertilization revealed that the correlation between segment and mRNA level is extremely significant ($P < 0.0001$), but that there is no effect of fertilization and time following fertilization ($P \approx 1$).

The mRNA profiles of 15 genes characterized in at least six eggs are shown in Figure 3A. The profiles fall into two distinct classes, and are characteristic of animal and vegetal locations, respectively. The mRNAs located preferentially at the animal pole are FoxH1, Oct60, GSK-3β, dishevelled, EF-1alpha, Xmam, Tcf-3, GAPDH, β-catenin and XPar-1. Those located at the vegetal pole are VegT, Vg1, Xdazl, Wnt11 and Otx1. In addition, Stat3 was measured in four cells and found to be located in the animal hemisphere, while Xcad2 (measured in four cells) and Deadsouth (measured in three cells) were vegetally located (data not shown). For Oct60 (animal) and Wnt11 (vegetal), the intracellular expression profiles measured by QPCR tomography were confirmed with digital PCR (Figure 4). Oct60 shows highest expression in Sections 2 and 3 from the animal pole, while Wnt11 expression is largest in Section 5, which is closest to the vegetal pole. Qualitatively, this is in agreement with the real-time PCR results in Figure 3. Assuming there are no important differences, we calculated the average vegetal and animal mRNA profiles also shown in Figure 3B. The data are based on 117 measured vegetal profiles and 166 measured animal profiles. The error bars represent ±1 SD, within which 68% of the measured values should be found. The standard errors of the means were insignificant, and the average values shown by the symbols have negligible errors.

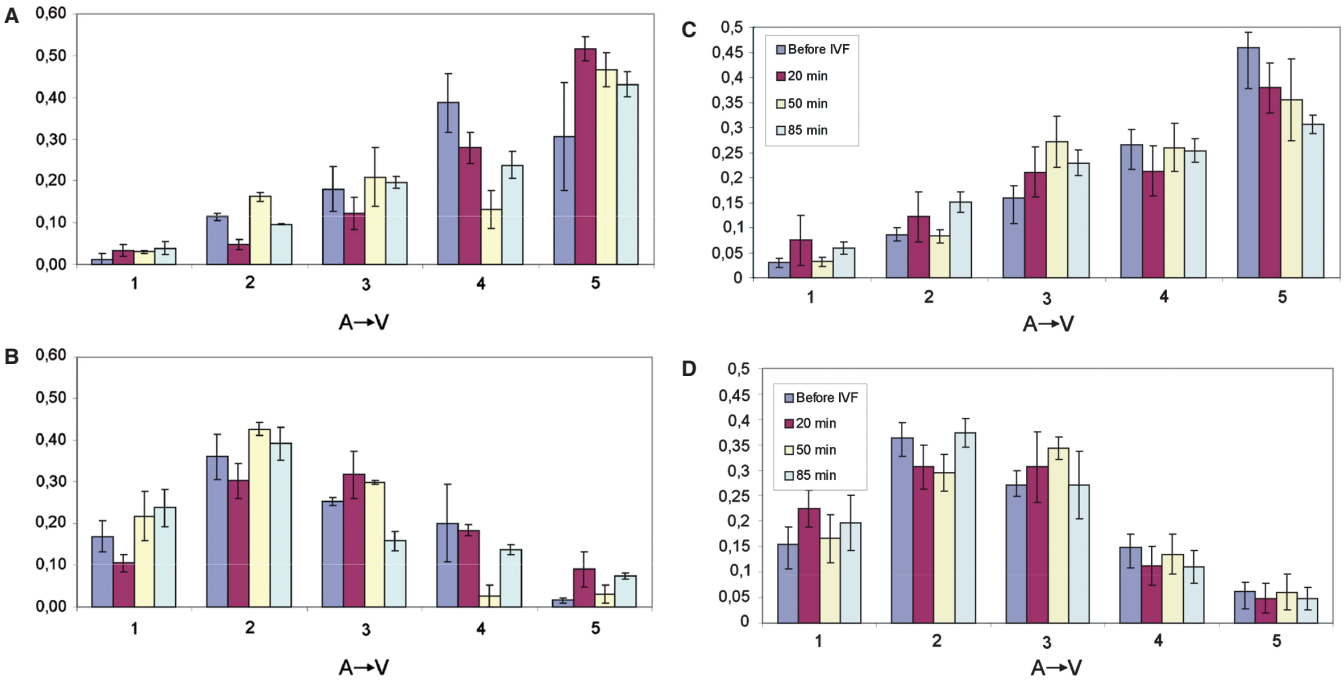

Figure 2. Intracellular gradients (A→V) of mRNA levels in *Xenopus laevis* oocytes. Distribution of (**A**) Vg1 and (**B**) Oct60 expression density along the oocyte animal–vegetal axis. The RNA was prepared from two to three individual eggs (standard error of the means indicated by error bars) from four different females (indicated by regular bars). Effect of fertilization. Distribution of (**C**) Vg1 and (**D**) Oct60 along the animal–vegetal axis. RNA was prepared from at least six eggs before IVF and at 20, 50 and 85 min after fertilization. Error bars indicate standard error of the means.

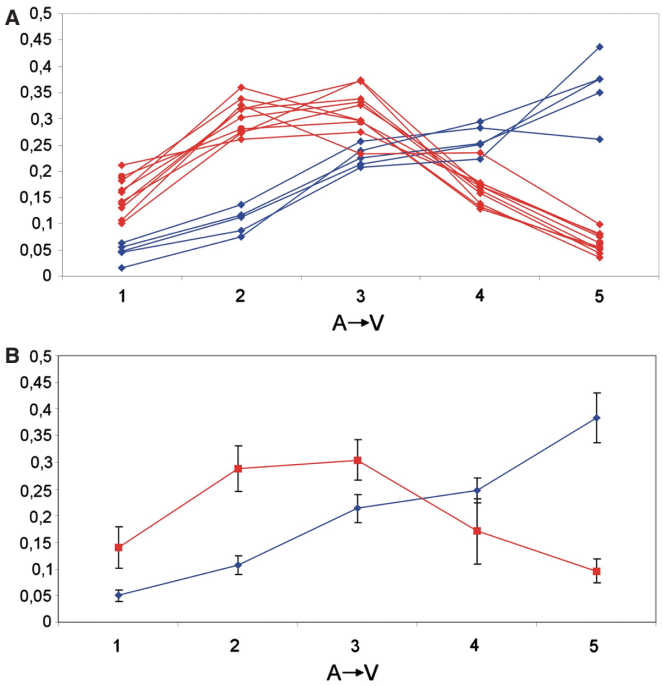

Figure 3. (**A**) Averaged intracellular mRNA concentration profiles (A→V) for genes studied in at least six eggs. Animal genes (FoxH1, Oct60, GSK-3β, dishevelled, EF-1alpha, Xmam, Tcf-3, GAPDH, β-catenin and XPar-1) are shown in red and vegetal genes (VegT, Vg1, Xdazl, Wnt11 and Otx1) are shown in blue. (**B**) Average expression profiles of all vegetal (red) and all animal (blue) genes. The error bars indicate 1 SD.

DISCUSSION

This is the first report of sub-cellular expression profiling and quantification of mRNA within a single cell. Using real-time PCR, which is currently the most sensitive and reliable technique for quantitative mRNA analysis, we measured the intracellular profiles of selected developmental mRNAs within the *X. laevis* oocyte. Our results reveal the existence of characteristic expression gradients, and demonstrate that real-time PCR tomography is highly suitable for measuring them quantitatively. Out of the 18 genes studied, 11 were found preferentially located at the animal pole (animal genes), while seven were preferentially located at the vegetal pole (vegetal genes). The 'animal genes' were FoxH1, Oct60, GSK-3β, dishevelled, EF-1α, Xmam, Tcf-3, GAPDH, β-catenin, XPar-1 and Stat3. Oct60 has previously been found located at the animal pole by *in situ* hybridization (10). EF-1α and GAPDH have been ascribed housekeeping functions and used as reference genes (20). However, they show clear animal location. Interestingly, APC, β-catenin, Fz7, GSK-3β, dishevelled and Tcf-3, which specify components of the Wnt pathway are animal genes, whereas Wnt11 itself shows vegetal location. Xmam and FoxH1 have not been localized previously. The genes found to have vegetal location were VegT, Vg1, Xdazl, Wnt11, Otx1, Deadsouth and Xcad2.

Within the resolution of our technique all genes contained in each of the two groups had comparable profiles. The animal genes were preferentially found in the

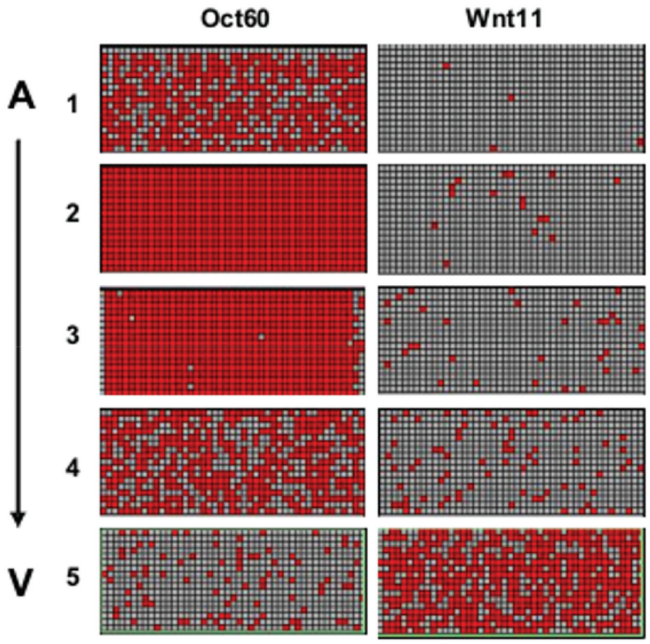

Figure 4. Digital PCR of Wnt11 and Oct60 showing abundance of transcripts in the five oocyte segments (A→V). mRNA from each segment was distributed into 765 chambers that were analyzed by RT-PCR. Red indicates positive PCR for targeted product.

second and third (central) sections of the oocytes, while the vegetal genes were found preferentially in the fourth and fifth sections. However, although the polarization of the vegetal genes is much stronger than the (opposite) polarization of the animal genes, that polarization is not total. About 5% of mRNA molecules of the vegetal genes were found in the first section taken from the opposite pole and another 10% in the second section (Figure 3B). Hence, the extreme polarization of both animal and vegetal genes seen by *in situ* hybridization techniques, where virtually all genes are located at either pole (9), is not supported by our observations. Instead our data suggest that although there is a distinct bias to the location of the mRNA, it is distributed more evenly. The reason for this discrepancy is unclear; however, we note that the cell nucleus is expected to be located in sections two and three, which is where we find the animal genes to be most abundant. Perhaps most of the animal mRNAs are still located within the nucleus and are held there until their translation is required. Interestingly, fertilization of the oocytes and the cortical rotation that follows has no detectable effect on the intracellular mRNA gradients.

In summary, real-time PCR tomography can measure intracellular mRNA gradients more sensitively and with greater resolution than traditional *in situ* hybridization. In the present work, each cell was cut into 35 30 µm slices, yielding up to 75 ng of RNA per slice. This is not close to any limit, since a regular cryostat can easily cut slices of 10 µm, yielding some 100 slices from a single *X. laevis* oocyte. This would allow the generation of mRNA profiles with much higher resolution, the only potential constraint being the amount of RNA extracted from each slice. However, the use of appropriate multiplexing and/or pre-amplification techniques should help overcome this limitation. Other applications of real-time PCR tomography are readily envisaged: the localization of nuclei through genomic DNA, of mitochondria through mitochondrial DNA and of translationally active sites through ribosomal RNA. The techniques can also be used to localize viruses and bacteria in tissue sections.

SUPPLEMENTARY DATA

Supplementary Data are available at NAR Online.

ACKNOWLEDGEMENTS

This work was supported by grant No. B500520601 project No. AVOZ 50520514 awarded by the AS CR, grant from the Swedish Research Council and by Carl Tryggers foundation. We are grateful to the charity Bowel and Cancer Research for support. We also thank Martin Pieprzyk for valuable help with digital PCR measurements. Funding to pay the Open Access publication charges for this article was provided by the Institutional Research Concept No. AV0Z50520701 of the Academy of Sciences of the Czech Republic.

Conflict of interest statement. None declared.

REFERENCES

1. Shav-Tal,Y. and Singer,R.H. (2005) RNA localization. *J. Cell. Sci.*, **118**(Pt 18), 4077–4081.
2. Danilchik,M.V. and Gerhart,J.C. (1987) Differentiation of the animal-vegetal axis in Xenopus laevis oocytes. I. Polarized intracellular translocation of platelets establishes the yolk gradient. *Dev. Biol.*, **122**, 101–112.
3. Heasman,J. (2006) Maternal determinants of embryonic cell fate. *Semin. Cell Dev. Biol.*, **17**, 93–98.
4. Gerhart,J.C., Vincent,J.P., Scharf,S.R., Black,S.D., Gimlich,R.L. and Danilchik,M. (1984) Localization and induction in early development of Xenopus. *Philos. Trans. R. Soc. Lond. B Biol. Sci.*, **307**, 319–330.
5. MacArthur,H., Bubunenko,M., Houston,D.W. and King,M.L. (1999) Xcat2 RNA is a translationally sequestered germ plasm component in Xenopus. *Mech. Dev.*, **84**, 75–88.
6. MacArthur,H., Houston,D.W., Bubunenko,M., Mosquera,L. and King,M.L. (2000) DEADSouth is a germ plasm specific DEAD-box RNA helicase in Xenopus related to eIF4A. *Mech. Dev.*, **95**, 291–295.
7. Chang,P., Perez-Mongiovi,D. and Houliston,E. (1999) Organisation of Xenopus oocyte and egg cortices. *Microsc. Res. Tech.*, **44**, 415–429.
8. Zhou,Y. and King,M.L. (2004) Sending RNAs into the future: RNA localization and germ cell fate. *Iubmb Life*, **56**, 19–27.
9. King,M.L., Messitt,T.J. and Mowry,K.L. (2005) Putting RNAs in the right place at the right time: RNA localization in the frog oocyte. *Biol. Cell*, **97**, 19–33.
10. Mowry,K.L. and Cote,C.A. (1999) RNA sorting in Xenopus oocytes and embryos. *FASEB J.*, **13**, 435–445.
11. Ossipova,O., He,X. and Green,J. (2002) Molecular cloning and developmental expression of Par-1/MARK homologues XPar-1A and XPar-1B from Xenopus laevis. *Mech. Dev.*, **119**(Suppl. 1), S143–S148.
12. Gerhart,J., Danilchik,M., Doniach,T., Roberts,S., Rowning,B. and Stewart,R. (1989) Cortical rotation of the Xenopus egg:

consequences for the anteroposterior pattern of embryonic dorsal development. *Development*, **107**(Suppl), 37–51.
13. Vincent,J.P. and Gerhart,J.C. (1987) Subcortical rotation in Xenopus eggs: an early step in embryonic axis specification. *Dev. Biol.*, **123**, 526–539.
14. Heasman,J., Kofron,M. and Wylie,C. (2000) Beta-catenin signaling activity dissected in the early Xenopus embryo: a novel antisense approach. *Dev. Biol.*, **222**, 124–134.
15. Wylie,C., Kofron,M., Payne,C., Anderson,R., Hosobuchi,M., Joseph,E. and Heasman,J. (1996) Maternal beta-catenin establishes a 'dorsal signal' in early Xenopus embryos. *Development*, **122**, 2987–2996.
16. Bengtsson,M., Stahlberg,A., Rorsman,P. and Kubista,M. (2005) Gene expression profiling in single cells from the pancreatic islets of Langerhans reveals lognormal distribution of mRNA levels. *Genome Res.*, **15**, 1388–1392.
17. Kubista,M., Andrade,J.M., Bengtsson,M., Forootan,A., Jonak,J., Lind,K., Sindelka,R., Sjoback,R., Sjogreen,B. *et al.* (2006) The real-time polymerase chain reaction. *Mol. Aspects Med.*, **27**, 95–125.
18. Nolan,T., Hands,R.E. and Bustin,S.A. (2006) Quantification of mRNA using real-time RT-PCR. *Nat. Protoc.*, **1**, 1559–1582.
19. Ståhlberg,A., Kubista,M. and Pfaffl,M. (2004) Comparison of reverse transcriptases in gene expression analysis. *Clin. Chem.*, **50**, 1678–1680.
20. Sindelka,R., Ferjentsik,Z. and Jonak,J. (2006) Developmental expression profiles of Xenopus laevis reference genes. *Dev. Dyn.*, **235**, 754–758.